Chemical Analysis of Spray Pyrolysis Gadolinia-Doped Ceria Electrolyte Thin Films for Solid Oxide Fuel Cells

Jennifer L. M. Rupp,*,† Tanja Drobek,‡ Antonella Rossi,§ and Ludwig J. Gauckler†

Institute of Nonmetallic Inorganic Materials and Laboratory for Surface Science and Technology, Department of Materials, Swiss Federal Institute of Technology, ETH Zurich, Wolfgang-Pauli-Strasse 10, CH-8093 Zurich, Switzerland, and Università degli Studi di Cagliari, Dipartimento di Chimica Inorganica ed Analitica, UdR INSTM, I-09100 Cagliari, Italy

Received June 22, 2006. Revised Manuscript Received November 24, 2006

Current solid oxide fuel cell research aims for the reduction of operating temperatures while maintaining power output to reduce the cost of operation. A promising strategy for achieving this goal is to replace common microcrystalline yttria-stabilized zirconia (YSZ) electrolytes of 10−200 μm thickness with nanocrystalline gadolinia-doped ceria electrolytes (CGO) of 100−500 nm thickness deposited by spray pyrolysis. While decreasing the electrolyte thickness, we expect ohmic losses of the fuel cell to decrease linearly and can realize lower operation temperatures at equal efficiency. In this study, the chemical homogeneity of as-deposited and annealed $Ce_{0.8}Gd_{0.2}O_{1.9-x}$ thin films deposited by spray pyrolysis at 350 °C and annealed at 1000 °C were investigated. The chemical composition of the gadolinia-doped ceria films was studied by X-ray photoelectron spectroscopy and Ar^+ sputtering as a function of film depth. After the topmost layer was removed by Ar^+ sputtering, the thin films showed a surprisingly homogeneous dopant concentration of 23.4 ± 0.6 at % gadolinia in ceria, independent of the film depth. However, spray-pyrolysis-related residues of the precursors (i.e., chlorine from the precursor salt, carbon from the pyrolysis solvents, and water) could be found at unexpected depths in the film and even after annealing at temperatures as high as 1000 °C. The pyrolytic decomposition of the spray pyrolysis thin films is not completely finished after deposition. Changes in the chemical composition may be present during solid oxide fuel cell operation of CGO electrolytes at 600−1000 °C.

1. Introduction

In recent years, the spray pyrolysis synthesis technique has been used widely for the preparation of solid oxide fuel cell (SOFC) electrolyte thin films. Such spray-pyrolysis-made thin films are advantageous compared to sintered electrolyte pellets or tapes because they can be made as thin as 100−500 nm, which decreases the ohmic resistance by a factor of 100 and consequently increases fuel cell power outputs.[1,2] Spray-pyrolyzed thin films also offer high film quality and low processing costs compared to conventional thin film preparation techniques such as pulsed laser deposition and chemical or physical vapor deposition. The superior quality of the SOFC electrolyte films made with spray pyrolysis is due to their dense and amorphous nature after deposition.[1,3] The amorphous state can be converted to a nanocrystalline isotropic microstructure by annealing without developing columnar grained microstructure with grain boundaries perpendicular to the film surface.[4]

Common thin film technologies such as pulsed laser deposition or physical vapor deposition result in crystalline microstructures that usually show columnar grains and texturing, resulting in unfavorable anisotropic electrical conductivity.[5] However, up to now, the chemical homogeneity assumed for spray-pyrolyzed thin films remains unproven. During spray pyrolysis deposition, a precursor solution of metal salts and solvents is sprayed as fine droplets onto a heated substrate.[6] When the droplets reach the heated substrate, they spread out and undergo pyrolytic decomposition.[7] Newly deposited flat droplets, with thicknesses in the 10−20 nm range, pile up on the previously deposited ones and undergo pyrolytic decomposition as well. This process continues until a film thicknesses of 100−500 nm is reached.[7] It is still controversial whether the pyrolysis process is complete after deposition of the thin film.[7−9] The degree of decomposition is determined by the relationship between the substrate temperature, the boiling point of the solvents, and the melting point of the salts used for the precursor. A

* Corresponding author. E-mail: jennifer.rupp@mat.ethz.ch.
† Institute of Nonmetallic Inorganic Materials, Swiss Federal Institute of Technology.
‡ Laboratory for Surface Science and Technology, Swiss Federal Institute of Technology.
§ Università degli Studi di Cagliari.

(1) Perednis, D.; Gauckler, L. J. *Solid State Ionics* **2004**, *166*, 229.
(2) Stoermer, A. O.; Rupp, J. L. M.; Gauckler, L. J. *Solid State Ionics* **2006**, *177*, 2075.
(3) Perednis, D.; Gauckler, L. J. *Proceedings of the 8th International Symposium on SOFCs* **2003**, *7*, 970.
(4) Rupp, J. L. M.; Infortuna, A.; Gauckler, L. J. *Acta Mater.* **2006**, *54*, 1721.
(5) Chen, L.; Chen, C. L.; Huang, D. X.; Lin, Y.; Chen, X.; Jacobson, A. J. *Solid State Ionics* 2004,*175*, 103.
(6) Patil, P. S. *Mater. Chem. Phys.* **1999**, *59*, 185.
(7) Perednis, D.; Wilhelm, O.; Pratsinis, S. E.; Gauckler, L. J. *Thin Solid Films* **2005**, *474*, 84.
(8) Wilhelm, O.; Pratsinis, S. E.; Perednis, D.; Gauckler, L. J. *Thin Solid Films* **2005**, *479*, 121.
(9) Wilhelm, O.; Madler, L.; Pratsinis, S. E. *J. Aerosol Sci.* **2003**, *34*, 815.

10.1021/cm061449f CCC: $37.00
Published on Web 02/08/2007

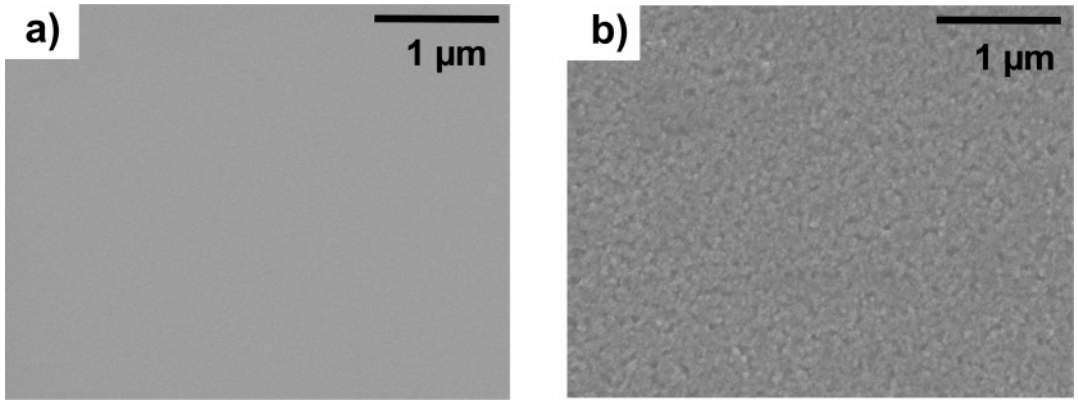

Figure 1. Microstructures of $Ce_{0.8}Gd_{0.2}O_{1.9-x}$ spray pyrolysis thin films (displayed in top views) for samples (a) as-deposited and (b) annealed at 1000 °C for 1 h.

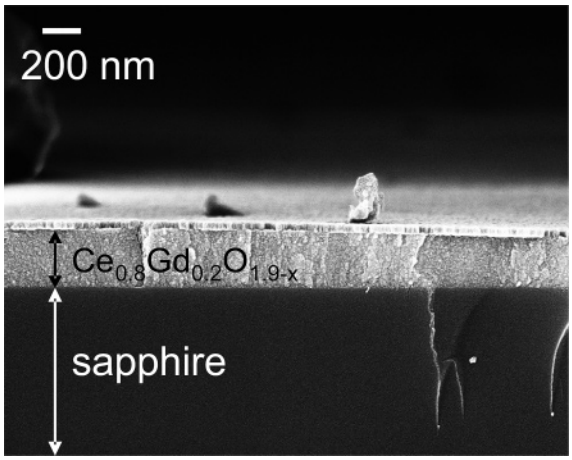

Figure 2. Microstructure of the cross section of a $Ce_{0.8}Gd_{0.2}O_{1.9-x}$ spray pyrolysis thin film on sapphire substrate after annealing. The top layer on the $Ce_{0.8}Gd_{0.2}O_{1.9-x}$ spray pyrolysis thin film is a sputtered platinum film added to avoid charging during SEM.

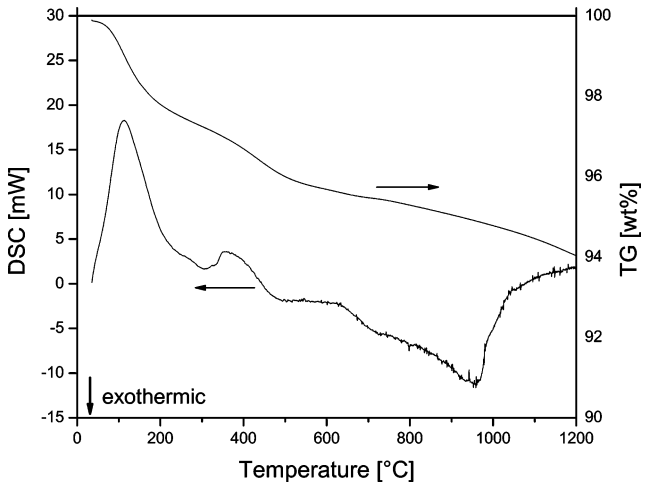

Figure 3. Differential scanning calorimetry (DSC) and thermogravimetry (TG) of a $Ce_{0.8}Gd_{0.2}O_{1.9-x}$ spray pyrolysis thin film.[4]

compromise has to be found between sufficiently high deposition temperatures to achieve complete decomposition if possible and the facility to deposit the droplets still in a wet state on the substrate for a piling up of the droplets.

An important property of the thin films is their chemical composition perpendicular to the film surface. The first droplets arriving on the heated substrate remain at temperature for a longer time than droplets deposited on top of the thin film. This might result in a gradient of the chemical

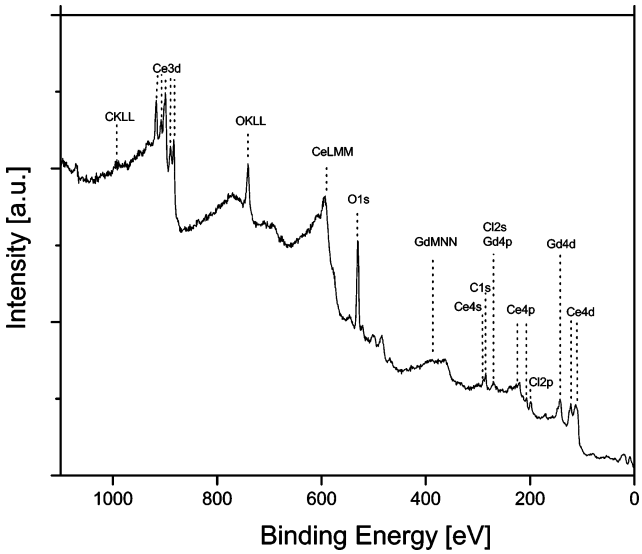

Figure 4. Survey X-ray photoelectron spectrum of the annealed $Ce_{0.8}Gd_{0.2}O_{1.9-x}$ spray pyrolysis thin film (1000 °C for 1 h, ±3 °C/min.). Ce, Gd, O, C, and Cl are detected in the spectrum.

composition and, therefore, a gradient of the amount of point defects, resulting in differences in the electrical conductivity essential for electrochemical devices, including fuel cells.

In this study, the chemical homogeneity of spray-pyrolyzed gadolinia-doped ceria SOFC electrolyte thin films was investigated. In addition, different annealing conditions were studied in order to investigate whether the pyrolytic decomposition was completed during the spray pyrolysis deposition of a gadolinia-doped ceria film or whether the films require additional annealing. We also want to address how the final chemical composition varied over the film thickness.

2. Experimental Section

2.1. Materials. The gadolinia-doped ceria (CGO) spray pyrolysis precursor solutions were made of 0.02 mol/L gadolinium chloride (Alfa Aesar, 99.9% purity) and 0.08 mol/L cerium nitrate (Alfa Aesar, 99% purity) dissolved in 33:33:33 vol % ethanol, diethylene glycol monobutyl ether and 1-methoxy-2-propanol (all solvents from Fluka, >99% purity). These precursor solutions were fed into a spray gun (Compact 2000KM, Bölhoff Verfahrenstechnik, Germany) with a liquid flow rate of 34.4 mL/h and atomized with 1.5 bar air pressure. The droplets produced in this manner were sprayed on a heated sapphire single-crystal substrate (Stettler, Switzerland) at 310 ± 10 °C for 5 h. The working distance between the spray

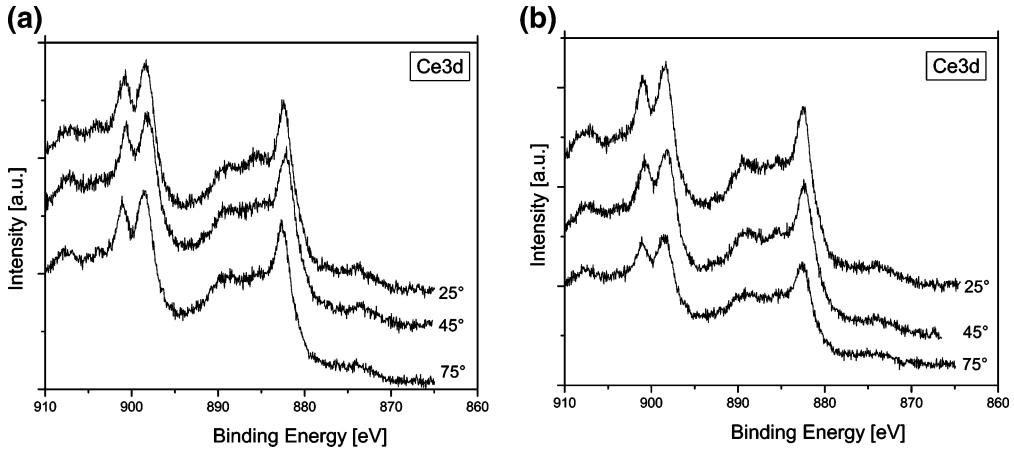

Figure 5. Angle-resolved Ce 3d X-ray photoelectron spectra of $Ce_{0.8}Gd_{0.2}O_{1.9-x}$ spray pyrolysis thin films for samples (a) annealed at 1000 °C for 1 h and (b) as-deposited.

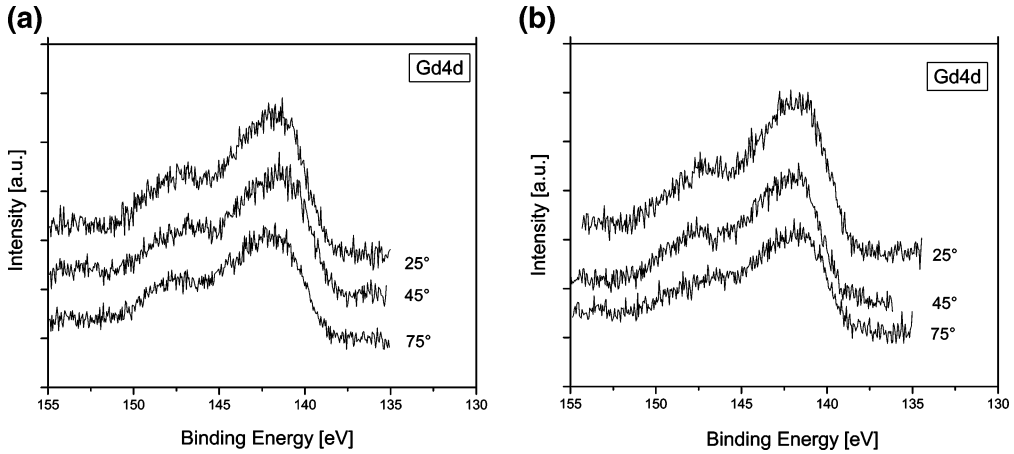

Figure 6. Angle-resolved Gd 4d X-ray photoelectron spectra of $Ce_{0.8}Gd_{0.2}O_{1.9-x}$ spray pyrolysis thin films for samples (a) annealed at 1000 °C for 1 h and (b) as-deposited.

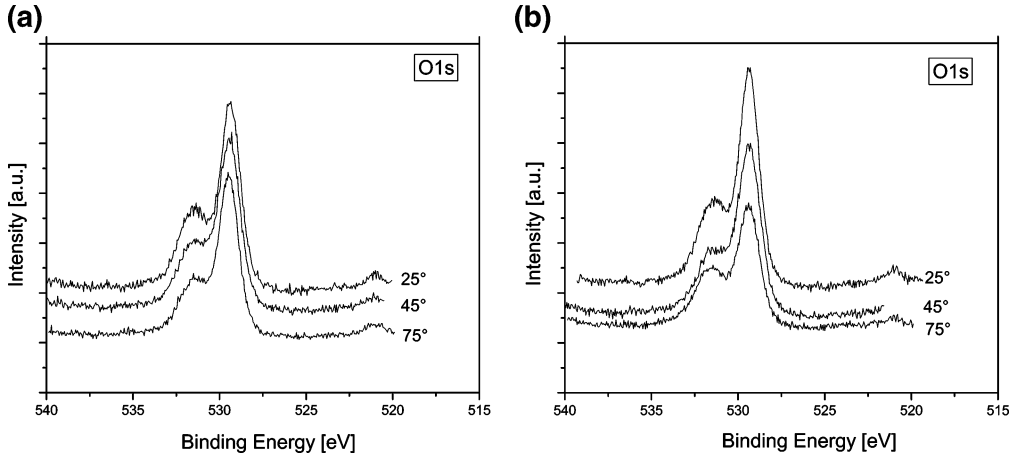

Figure 7. Angle-resolved O 1s X-ray photoelectron spectra of $Ce_{0.8}Gd_{0.2}O_{1.9-x}$ spray pyrolysis thin films for samples (a) annealed at 1000 °C for 1 h and (b) as-deposited.

nozzle and the hot plate was kept at 45 cm during all experiments. The spray pyrolysis process is described in further detail elsewhere.[1,6,8,9] To study the influence of annealing on the thin film chemistry, we heated and cooled the as-deposited films at a rate of 3 °C/min to 1000 °C with an isothermal hold of 1 h. For chemical characterization, the compositions of the annealed samples were compared with those of as-deposited samples, which did not undergo any further heat treatment after the pyrolysis during deposition.

2.2. Methods. Energy-Dispersive X-ray Spectroscopy. The microstructure of the thin films was characterized using scanning electron microscopy (SEM, Leo 1530, Germany). The top layers of the thin films were sputtered (Bal-Tec, SCD 050, Sputter Coater) with a platinum coating to allow for imaging at higher resolutions.

The chemical composition was determined by energy-dispersive X-ray spectroscopy (EDX, Leo 1530, Germany) using the cerium and gadolinium L-lines at 20 kV. For quantitative EDX analysis, the Proza correction method was chosen.

Differential Scanning Calorimetry and Thermogravimetry. Differential scanning calorimetry and thermogravimetry measurements (DSC/TG, Netzsch STA 449C) were performed. For this purpose, as-deposited thin films were scratched off the substrate and the

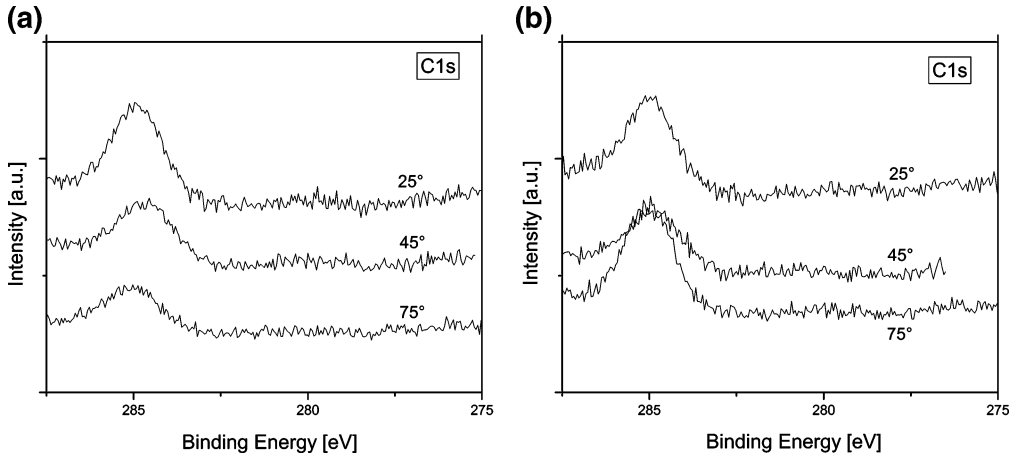

Figure 8. Angle-resolved C1s X-ray photoelectron spectra of $Ce_{0.8}Gd_{0.2}O_{1.9-x}$ spray pyrolysis thin films for samples (a) annealed at 1000 °C for 1 h and (b) as-deposited.

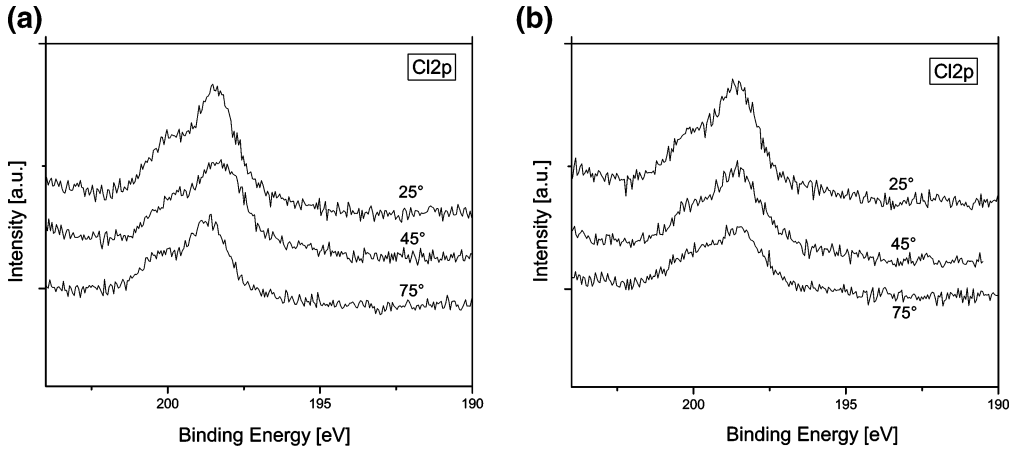

Figure 9. Angle-resolved Cl2p X-ray photoelectron spectra of $Ce_{0.8}Gd_{0.2}O_{1.9-x}$ spray pyrolysis thin films for samples (a) annealed at 1000 °C for 1 h and (b) as-deposited.

powder (with an original mass of 126.24 mg) was heated during DSC/TG from room temperature to 1200 °C at 10 °C/min in air. Outgassing species attributed to mass losses during TG were detected with a mass spectrometer (M Balzers Quadstar 422).

X-ray Photoelectron Spectroscopy. X-ray photoelectron spectra were acquired using a PHI 5700 (Physical Electronics Inc., Eden Prairie, MN) from uncoated film surfaces. The residual pressure during the analysis was 1×10^{-7} Pa. The measurements were carried out using a Mg Kα (1253.6 eV) radiation source run at 400 W. The incident angle was 54.7° and the emission angle was 45° with respect to the sample surface normal. All the spectra were obtained in digital mode. The lens system was OMNIFOCUS IV and the spectrometer was run in the minimum area mode, defining an analyzed spot size of 0.4 mm in diameter. A constant pass energy of 23.5 eV through the hemispheres of the electron analyzer, operated in the fixed analyzer transmission (FAT) mode, was used for the narrow-scan of Ce 3d, Gd 4d, O 1s, Cl 2p, and C 1s. The wide-scan spectra were acquired with a pass energy of 117.4 eV.

The instrument was calibrated using the inert-gas-ion-sputter-cleaned reference materials SCAA90 of Cu, Ag, and Au.[10] The accuracy of the binding energy values was found to be ±0.05 eV. Sample charging was corrected by referring all binding energies to the carbon 1s signal at 285.0 eV.

Angle-resolved XPS measurements were carried out at 25, 45, and 75° takeoff angles relative to the sample surface.

Depth Profiling. The ion gun instrumentation was Physical Electronics 04-303A (detector parameters as described above). The ion composition for depth profiling was Ar^+, and a kinetic energy of 3 keV was used. At the latter kinetic energy, an unrastered spot size of 0.25 mm was present. The typical raster size was 9×9 mm^2. The relative sputter rate was determined by performing an experiment using the same experimental conditions on a SiO_2 thin film sample of known thickness. All XPS spectra measured to determine the depth profile composition were carried out with a takeoff angle of 45°.

Data Processing. The peaks were resolved in their Gaussian−Lorentzian components after Shirley−Sherwood background subtraction[11] using Casa XPS software.[12]

The energy doublet separation was constrained and set at 5 eV for Gd $4d_{5/2}$−Gd $4d_{3/2}$,[13,14] 18.4 eV for partially reduced Ce $3d_{5/2}$−Ce $3d_{3/2}$,[15,16] and 18.2 eV for mainly reduced ceria Ce $3d_{5/2}$−Ce $3d_{3/2}$.[16] The relative intensities of each doublet were taken equal to the 3:2 $d_{5/2}$:$d_{3/2}$ ratio.[17] Because of the extreme binding energy shifts of the Ce 3d spectra, one peak of Ce $3d_{3/2}$ is missing in the spectra. The gadolinium satellite in the C 1s and the cerium satellite in the Cl 2p spectra were subtracted for analysis. The atomic ratios of

(10) ISO 15472:2001 2001.

(11) Shirley, D. A. *Phys. Rev. B* **1972**, *5*, 4709.
(12) Fairley, N. *CASA XPS*, version 2.0; CASA Software Ltd.: Devon, U.K.
(13) Terzieff, P.; Lee, K. J. *Appl. Phys.* **1979**, *50*, 3565.
(14) Uwamino, Y.; Ishizuka, T.; Yamatera, H. *J. Electron Spectrosc. Related Phenom.* **1984**, *34*, 67.
(15) Rao, M. V.; Shripathi, T. *J. Electron Spectrosc. Related Phenom.* **1997**, *87*, 121.
(16) Paparazzo, E. *Surf. Sci. Lett.* **1990**, *234*, L253.
(17) Briggs, D; Seah, M. P. *Practical Surface Analysis*; J. Wiley: New York, 1990.

Table 1. X-ray Photoelectron Spectroscopy Binding Energies (BE) and Full Width at Half-Maximum (fwhm) for the Investigated Annealed Gadolinia-Doped Ceria Thin Film

	Ce $3d_{5/2}$	Ce $3d_{3/2}$	Gd $4d_{5/2}$	Gd $4d_{3/2}$	O 1s	C 1s	Cl 2p	etching time/etched reference depth of SiO_2
BE (fwhm) (eV)	882.2 (2.6) (v)	900.6 (2.6) (u)	141.9 (4.2)	146.7 (5.5)	529.5 (2.1)	285(2.3)	201.8 (2.7)	
	883.5 (3.5) (v')	901.9 (3.5) (u')			531.7 (2.2)			0 min etched/0 nm deep in SiO_2
	888.6 (4.8) (v'')	907.1 (4.8) (u'')			533.6 (2.2)			
	898.2 (2.4) (v''')	916.7 (2.4) (u''')						
BE (fwhm) (eV)	880.9 (3.3) (v_0)	899.1 (3.3) (u_0)	141.4 (4.0)	146.4 (5.5)	529.3 (2.2)		201.9 (3.3)	8.67 min etched/103 nm deep in SiO_2
	885.4 (4.0) (v')	903.5 (4.0) (u')						
	895.1 (3.8) (v''')	913.3 (3.8) (u''')			532.1 (1.9)			

Table 2. EDX and XPS Analysis of the As-Deposited and Annealed Gadolinia-Doped Ceria Spray Pyrolysis Thin Films (standard deviations were calculated over experiments)

	EDX analysis		XPS analysis after sputtering time[a]	
gadolinia-doped ceria thin film	Ce:Gd for Ce (%)	Ce:Gd for Gd (%)	Ce:Gd for Ce (%)	Ce:Gd for Gd (%)
as-deposited	76.2 ± 1.1	23.8 ± 1.4	76.6 ± 0.6	23.4 ± 0.6
annealed at 1000 °C for 1 h (with 3 °C/min)	75.4 ± 1.8	24.6 ± 2.5	77.4 ± 0.6	22.6 ± 0.6

[a] Refers to 10 nm sputtered depth in SiO_2.

Table 3. Literature Comparison of the X-ray Photoelectron Spectroscopy Binding Energies (BE) for Gd 4d Shells

spray pyrolysis annealed $Ce_{0.8}Gd_{0.2}O_{1.9-x}$ thin film at 1000 °C (this study)		sintered Gd_2O_3 pellet[13]		sintered Gd_2O_3 pellet[35]	
Gd $4d_{5/2}$	Gd $4d_{3/2}$	Gd $4d_{5/2}$	Gd $4d_{3/2}$	Gd $4d_{5/2}$	Gd $4d_{3/2}$
142.0	146.7	141.6	146.7	142.5	147.9

the elements present in the film were calculated from areas corrected for Scofield photoionization cross-sections,[18] the transmission function of the instrument,[19] and the inelastic main free paths.[20]

3. Results

3.1. Thin Film Characterization. After spray pyrolysis deposition, the CGO thin films are amorphous and crystallize at temperatures higher than 500 °C during annealing.[4] The top-view SEM microstructures of the CGO spray pyrolysis thin films are displayed in Figure 1 for the (a) as-deposited and (b) annealed thin films. The as-deposited thin film was amorphous with no grains visible in the SEM micrograph (Figure 1a), whereas the annealed thin film was crystalline with typical grain sizes below 100 nm (Figure 1b). In previous experiments on crystallization and grain growth of this type of thin film, an average grain size of 60 nm was measured for CGO films synthesized with spray pyrolysis and thermally treated as given here.[4]

The cross-sectional view of the annealed CGO thin film (Figure 1b) is presented in Figure 2. Even after annealing at elevated temperatures, spray-pyrolyzed CGO thin films remain crack- and pore-free. From the micrograph of the cross section (Figure 2), we determined a film thickness of 270 nm. The thin layer on top of the cerium gadolinium oxide is due to a sputter-deposition layer of platinum that was added to avoid charging effects during SEM measurements.

3.2. Bulk Chemical Characterization. The chemistry of the gadolinia-doped ceria spray pyrolysis thin films as a function of temperature with DSC and TG measurements was previously presented.[4] To compare the DSC/TG analysis to the XPS results given in this section, we briefly summarize the results of ref 4: In Figure 3, the thermal signal and the weight change are shown versus temperature from the DSC/TG run. Upon heating, a pronounced endotherm with a maxima at 180 °C occurs, accompanied by a mass loss of ~3 wt %, and is assigned to desorption of water. Between 400 and 1000 °C, there is a broad exotherm coincident with a mass loss of 2 wt %. This may be caused by heat release due to crystallization from the amorphous material.[4,21] In addition, outgassing water and carbon was detected at temperatures up to 1000 °C by mass spectrometry during the heating. The carbon content in the thin film is a residue of the organic precursor solvent used during the spray pyrolysis process. At high temperatures of 1000−1200 °C, the mass loss as detected by TG is still not completed. This mass loss cannot be ascribed to water or carbon loss by mass spectrometry within this temperature regime.

Table 4. Initial States and Final States of Ce^{3+} and Ce^{4+} Ions in Ce 3d Core Level X-ray Photoelectron Spectroscopy Spectra[34] (V denotes the valance band, lines belonging to Ce $3d_{3/2}$ are labeled with u, and lines belonging to Ce $3d_{5/2}$ are labeled with v)

ion	initial state	final state
Ce^{3+}	$3d^{10}4f^1$	v^0, u^0: $3d^94f^2V^{n-1}$
	$3d^{10}4f^1$	v', u': $3d^94f^1V^n$
	$3d^{10}4f^0$	v, u: $3d^94f^2V^{n-2}$
Ce^{4+}	$3d^{10}4f^0$	v'', u'': $3d^94f^1V^{n-1}$
	$3d^{10}4f^0$	v''', u''': $3d^94f^0V^n$

Residues from the originally used pyrolysis salts such as chlorine (from gadolinium chlorine salt) and nitrogen (from cerium nitrate salt) were not detected by mass spectrometry during DSC/TG. The total mass loss is 6.34 wt % and can be attributed to outgassing water and residual carbon in the spray pyrolysis films.

3.3. Surface Analytical Characterization. In Figure 4, the X-ray photoelectron spectroscopy survey spectrum of the annealed spray pyrolysis CGO thin film is shown. In the survey spectrum, only the signals of cerium, gadolinium,

(18) Scofield, J. H. *J. Electron Spectrosc. Related Phenom.* **1976**, *8*, 129.
(19) Berresheim, K.; Matternklosson, M.; Wilmers, M. *Fresenius J. Anal. Chem.* **1991**, *341*, 121.
(20) Seah, M. P.; Dench, W. A. *Surf. Interface Anal.* **1979**, *1*, 2.
(21) Rupp, J. L. M.; Solenthaler, C.; Gasser, P.; Muecke, U. P.; Gauckler, L. J. *Acta Mater.* **2006**, in press.

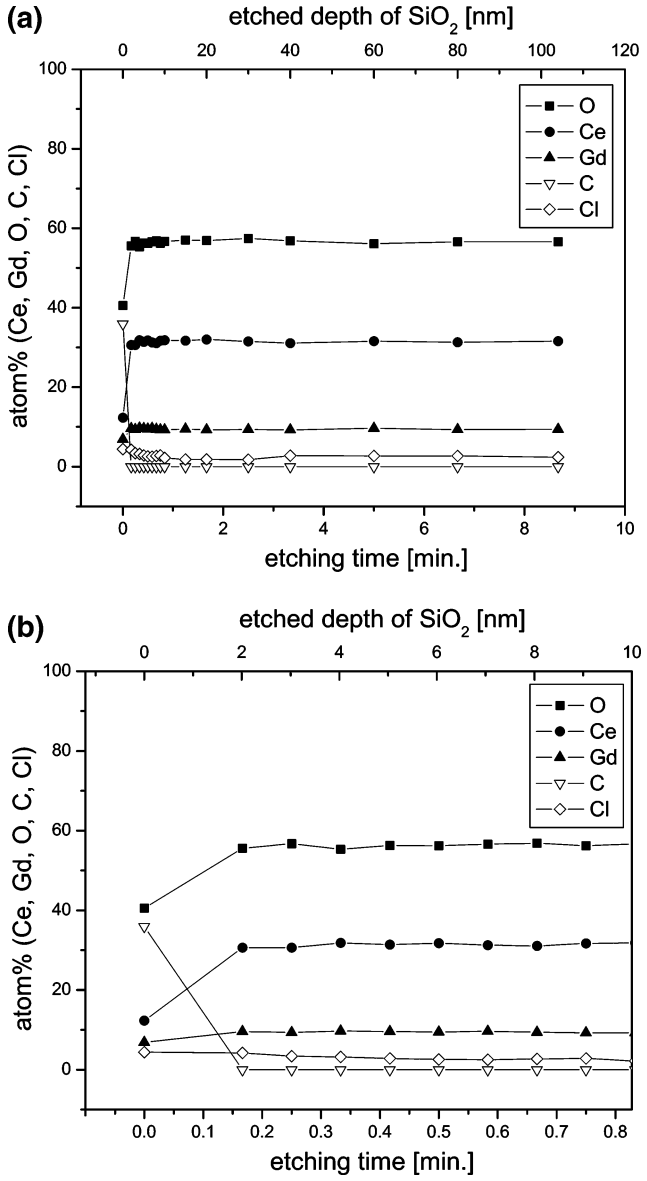

Figure 10. Depth profiling of a $Ce_{0.8}Gd_{0.2}O_{1.9-x}$ annealed spray pyrolysis thin film with Ar^+ for cerium, gadolinium, oxygen, carbon, and chlorine displayed for (a) the sputtered depth around 100 nm relative to SiO_2 and (b) the sputtered depth of the first 10 nm relative to SiO_2. The film was annealed at 1000 °C for 1 h, ±3 °C/min, prior to XPS measurements.

oxygen, chlorine, and carbon are visible. No additional impurities or contaminations were detected.

Angle-resolved photoelectron spectroscopy spectra provide information about whether the probed elements are surface contaminants or are related to the bulk chemistry. In Figures 5−9, detailed high-resolution spectra of Ce 3d, Gd 4d, O 1s, C 1s, and Cl 2p core levels at 25, 45, and 75° takeoff angles are shown. Figures 5 and 6 display the cerium 3d and gadolinium 4d spectra, respectively. For both elements, no distinct variation of the spectra with the takeoff angle was observed. Therefore, cerium and gadolinium can clearly be attributed to the bulk composition of the film. However, a weak angle dependence can partially be acknowledged for oxygen and a more pronounced one is visible for carbon and chlorine. The oxygen 1s signal can be resolved using three Gaussian−Lorentzian model functions, where the main peak at a binding energy of 529.5 eV refers

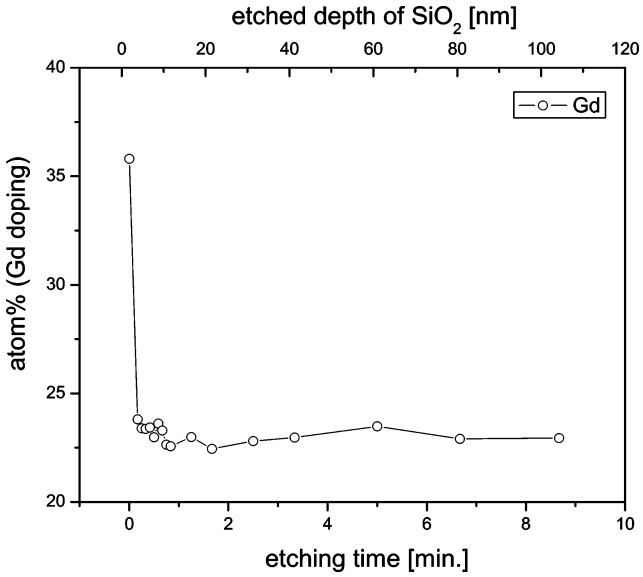

Figure 11. X-ray photoelectron spectroscopy depth profile for a $Ce_{0.8}Gd_{0.2}O_{1.9-x}$ annealed spray pyrolysis thin film sputtered with Ar^+ for gadolinium doping in ceria. The film was annealed at 1000 °C for 1 h, ±3 °C/min, prior to the XPS measurements.

to the lattice oxygen of the gadolinia-doped ceria[22] being independent from the takeoff angle, as shown in Figure 7. The peaks at 531.7 and 533.86 eV show an angle dependency and can be ascribed to hydroxyl groups and water.[23] In the literature, it is reported that a high affinity of cerium atoms to hydroxyl groups by hydrogen bonding and direct bonds occurs.[24,25] The carbon 1s peak shows a strong angle dependence, with a highest intensity at the lowest angle of 25° (see Figure 8). In Figure 9, the angle dependence of the chlorine 2p peak can be observed.

Thus, it can be concluded that the carbon is located on top of the thin films and coming from the environment, whereas the chlorine is enriched in the near-surface region below the carbon layer and results from film deposition.

The angle-resolved XPS observations on cerium, gadolinium, oxygen, carbon, and chlorine hold for the annealed as well as for the as-deposited sample.

A series of XPS spectra were collected in alternation with sputtering the surface with Ar^+ ions. In Figure 10, a depth profile of the atomic composition of the annealed CGO spray pyrolysis film is shown. The spectrum includes the data for cerium, gadolinium, oxygen, carbon, and chlorine. The binding energies and full width at half-maximum (fwhm) data of the components measured before sputtering and at the end of the sputtering procedure of the as-deposited thin film are presented in Table 1. The depth-profiling XPS experiment reveals that carbon is mainly detected as a surface-bound layer of adventitious carbon that disappears after the first sputter cycle (0.167 s of sputtering, 2 nm relative to SiO_2). This observation agrees with the strong

(22) Paparazzo, E.; Ingo, G. M.; Zacchetti, N. *J. Vac. Sci. Technol., A* **1991**, *9*, 1416.
(23) Borchert, H.; Forolova, Y. V.; Kaichev, V. V.; Prosvirin, I. P.; Alikina, G. M.; Lukashev, A. I.; Zaikovskii, V. I.; Moroz, E. M.; Trukhan, S. N.; Ivanov, V. P.; Paukshtis, E. A.; Bukhtiyarov, V. I.; Sadykov, V. A. *J. Phys. Chem. B* **2005**, 5728.
(24) Kim, S.; Merkle, R.; Maier, J. *Solid State Ionics* **2003**, *161*, 113.
(25) Prin, M.; Pijolat, M.; Soustelle, M.; Touret, O. *Thermochim. Acta* **1991**, *186*, 273.

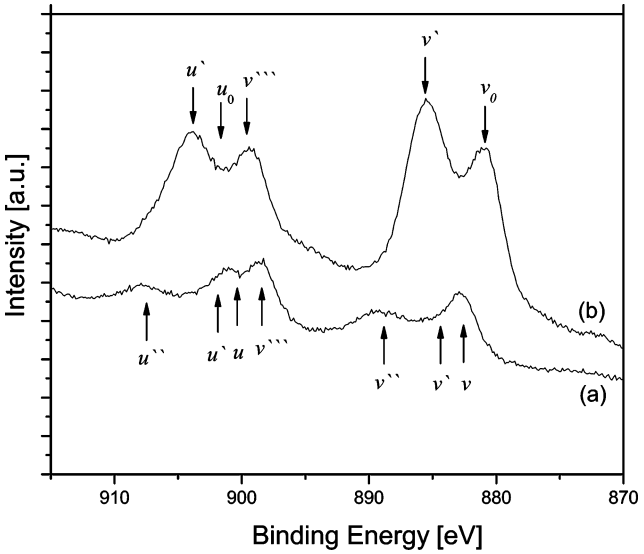

Figure 12. X-ray photoelectron spectra of annealed $Ce_{0.8}Gd_{0.2}O_{1.9-x}$ spray pyrolysis thin films for the Ce 3d doublet structures (a) without sputtering (b) after 102 sputter cycles (102 nm sputtered depth referred to SiO_2). In these spectra, the Ce 3d doublets v_0u_0, vu, $v'u'$, $v''u''$, and v''' without u''' are displayed. Peak of different cerium oxidation states can be assigned comparing the states of Table 4. The film was annealed at 1000 °C for 1 h, ×b1±3 °C/min, prior to XPS measurements.

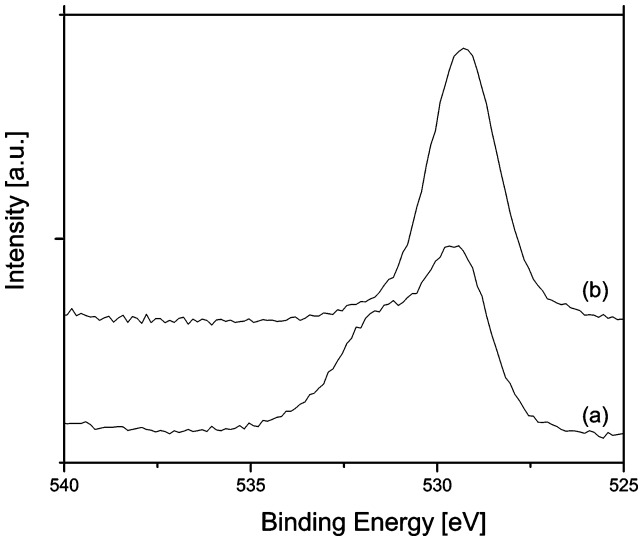

Figure 13. X-ray photoelectron spectra of annealed $Ce_{0.8}Gd_{0.2}O_{1.9-x}$ spray pyrolysis thin films for the O 1s core level (a) without sputtering and (b) after 102 sputter cycles (102 nm sputtered depth referred to SiO_2). The film was annealed at 1000 °C for 1 h, ±3 °C/min, prior to XPS measurements.

angle dependence of the peak area in the carbon 1s angle-resolved spectra in Figure 8.

Chlorine shows a slightly different depth distribution. From the data obtained before sputtering, an atomic concentration of 4.4 at % chlorine can be determined. The amount of chlorine decreases within several sputter cycles. After 8.7 min of sputtering (104 nm relative to SiO_2), the atomic concentration reached a plateau at 2.4 at %.

After the first sputter cycle, the concentration of gadolinia doping in the ceria lattice of the sample did not depend on the sputtering depth. The gadolinia doping is displayed in Figure 11. It is homogeneous over the whole probed depth profile, with a doping of 22.6 ± 0.6 at % gadolinia in the ceria lattice. In Table 2, this result is compared to the 24.6 ± 2.5 at % gadolinia in ceria determined by EDX. The original spray pyrolysis precursor should result in 20 at % gadolinia doping, but it is known that slight changes of the chemical composition can occur during the pyrolysis process at film deposition.[6] The detailed listing of the binding energies in comparison with data from the literature is given in Table 3.

Although the atomic concentration of cerium did not vary with sputtering depth, the spectra of the Ce 3d region did change distinctly during sputtering. In Figure 12, the spectra obtained before and after sputtering to a depth that refers to 102 nm in SiO_2 are compared. In the Ce 3d region, a number of lines are distinguishable, resulting from the multiplet splitting of the $3d_{3/2}$ and $3d_{5/2}$ energy levels. However, the cerium in the sample exists in different oxidation states that show distinct shifts in the binding energies. To clarify the origin of the different structures, lines belonging to Ce $3d_{3/2}$ are labeled with u and lines belonging to Ce $3d_{5/2}$ are labeled with v. In Table 4, the initial and final states of Ce^{3+} and Ce^{4+} ions in the Ce 3d core level and their peak assignment are given in reference to Pfau and Schierbaum.[34] Peak assignment for Ce 3d is presented in Figure 12 in accordance to Table 4.

It can be deduced that with increasing sputter time, the Ce 3d valence band structure of ceria changes from sub-stoichiometric Ce^{4+}/Ce^{3+}, which is partially oxidized, to mostly reduced ceria after sputtering. The Ce^{3+} related u_0v_0 doublet appears and the $u'v'$ doublet increases, whereas the Ce^{4+} related uv doublet and $u''v''$ doublet disappear with increasing sputter time and progressing reduction of the ceria.[27] In Tables 5 and 6, the binding energies deduced from the cerium 3d XPS signals of the annealed spray pyrolysis films are compared to spectra obtained on ceria ceramic pellets. There is good agreement of our data of binding energies and line widths with the literature.

In Figure 13, the oxygen 1s core level spectra before and after sputtering to a 102 nm depth in reference to SiO_2 are shown. The corresponding binding energies are listed in Table 1. With increasing sputter time, the lattice oxygen peak around 529.3 eV becomes stronger, whereas the oxygen peaks ascribed to adsorbed hydroxyl groups around 531.6 eV diminish. The contribution attributed to water at 533.76 eV completely disappears. These observations are consistent with the results of the angle-resolved XPS data of the O 1s region (Figure 7), which show the same trend.

In Table 7, the influence of annealing on the atomic composition of the spray pyrolysis thin films is displayed. The data were obtained from the annealed thin film sample after sputtering to a 10 nm depth relative to SiO_2. These data are essentially the same for the as-deposited thin film sample. It can be concluded that within the experimental error, the cerium to gadolinium ratio as well as the cerium and gadolinium to oxygen ratio are similar for both sample

(26) Reddy, B. M.; Khan, A.; Yamada, Y.; Kobayashi, T.; Loridant, S.; Volta, J.-C. *Langmuir* **2003**, *19*, 3025.
(27) Zhang, F.; Wang, P.; Koberstein, J.; Khalid, S.; Chan, S.-W. *Surf. Sci.* **2004**, *563*, 74.
(28) Pfau, A.; Schierbaum, K. D.; Göprel, W. *Surf. Sci.* **1995**, 1479.
(29) Venezia, A. M.; Pantaleo, G.; Longo, A.; Di Carlo, G.; Casaletto, M. P.; Liotta, F. L.; Deganello, G. *J. Phys. Chem. B* **2005**, 2821.

Table 5. Literature Comparison of the X-ray Photoelectron Spectroscopy Binding Energies (BE) for Ce 3d Shells in Ceramics with Partially Reduced Ceria

spray pyrolysis annealed $Ce_{0.8}Gd_{0.2}O_{1.9-x}$ thin film at 1000 °C (this study)		sintered CeO_2 pellet[15]		sintered CeO_2 pellet[14]	
Ce $3d_{5/2}$	Ce $3d_{3/2}$	Ce $3d_{5/2}$	Ce $3d_{3/2}$	Ce $3d_{5/2}$	Ce $3d_{3/2}$
882.2 (v)	900.6 (u)	882.1	900.6	882.4 (v)	900.4 (u)
883.5 (v')	901.9 (u')	885.2	903.8	885.4 (v')	903.9 (u')
888.6 (v'')	907.1 (u'')	888.5	907.2	888.6 (v'')	906.4 (u'')
898.2 (v''')	916.7 (u''')	898.2	916.5	898.5 (v''')	916.6 (u''')

Table 6. Literature Comparison of the X-ray Photoelectron Spectroscopy Binding Energies (BE) for Ce 3d Shells in Ceramics with Mainly Reduced Ceria

spray pyrolysis annealed $Ce_{0.8}Gd_{0.2}O_{1.9-x}$ thin film at 1000 °C (this study)		sintered Ce_2O_3 pellet[15]	
Ce $3d_{5/2}$	Ce $3d_{3/2}$	Ce $3d_{5/2}$	Ce $3d_{3/2}$
880.9 (v_0)	899.1 (u_0)	880.9	899.7
885.4 (v')	903.5 (u')	885.3	903.8
895.1 (v''')	913.3 (u''')		

treatments (see also Table 2), independent of annealing. An oxygen to cerium and gadolinium ratio of around 1.4 was determined for both samples. It reflects the reduced state of the ceria after sputtering.[30]

4. Discussion

Chemical Composition. The EDX analysis and the quantitative analysis of the XPS data both reveal the same chemical composition of $Ce_{0.77}Gd_{0.23}O_{1.9-x}$ for the annealed sample as well as the as-deposited sample (see Table 7). In both cases, the composition slightly differs from the ratio of the components in the precursor, which was prepared for $Ce_{0.80}Gd_{0.20}O_{1.9-x}$. This modification of the dopant concentration during the pyrolysis process is systematic and was already observed in previous studies.[6] For the preparation of a thin film with a specific composition, this outcome has to be taken into account.

Spray-Pyrolysis-Related Impurities. In contrast to other thin film preparation techniques, the pyrolysis process leads to thin films that contain trace amounts of carbon and hydroxyl groups from the precursors. It is interesting to note that in the case of water, organic solvents, and chlorine, these traces do not alter the electrical properties of the thin films considerably,[24,31,32] because the conductivity of the film is mainly determined by the dopant level, the strain in the grains, and the amount of grain boundaries (grain size).

The thin film samples that were the object of this study were prepared with a precursor containing gadolinium chloride and cerium nitrate in an organic solvent mixture. Nitrogen was not detected by mass spectroscopy applied in the DSC/TG experiment or by XPS analysis. DSC/TG experiments of cerium nitrate and gadolinium chloride salts showed that the decomposition temperature of the cerium nitrate is around 350 °C, close to the spray pyrolysis temperature of the substrate, whereas the gadolinium chloride has a higher decomposition temperature of around 690 °C. Although the high decomposition temperature of chlorine salts lead to chlorine residues in the films, chlorine salts have the ability to hinder the crystallization of the initially amorphous spray-pyrolyzed films at deposition temperatures[7] and are therefore a compromise to produce intact and crack-free films. Chlorine was not detected in the DSC/TG analysis, but was clearly visible in the XPS spectra. From the angle-resolved spectra and the sputtering profiles, it can be revealed that the chlorine is enriched in the near-surface region of the film. The concentration decreases within the outermost 10 nm to a value of about 2 at % in the bulk. In the as-deposited thin film, the concentration of chlorine decreases within the outermost 10 nm to a value of about 5 at % in the bulk. The segregation of chlorine to the surface of the thin films could be caused by the shorter process time for the pyrolysis of the topmost layers compared to the near-substrate layers at the bottom of the film. The reason why chlorine was not found in the DSC/TG analysis could be due to the fact that the total amount of chlorine in the film is very small and to the high decomposition temperature of gadolinium chloride. It is very likely that the rate of chlorine desorption during heating was below the detection limit.

In the case of carbon, a considerable amount of residue was detected in the DSC/TG analysis. It was desorbed from the film at elevated temperatures in air as detected by mass spectrometry. In the XPS measurements, carbon was found only in the topmost layers of the film, and could not be detected after sputtering. It is possible that the carbon residues in the film were too volatile to stay in the sample under the ultrahigh vacuum conditions and the Ar^+ ion bombardment applied for the XPS experiments.

Water was detected with both techniques. In the DSC/TG measurement, the desorption of water could be observed over a wide temperature range by mass spectrometry. The XPS analysis showed that the water was accumulated at the topmost 10−20 nm. The water was mainly visible as bound OH groups in the oxygen 1s spectra. It can be concluded from DSC/TG coupled with mass spectrometry experiments that even after thermal treatment at 1000 °C, there is still a significant amount of water remaining in the film after pyrolysis.

From the careful analysis of the traces, their spatial distribution, and alteration due to heat treatment, it can be concluded that the spray pyrolysis process is not finished after the deposition of the last precurser droplets, but a considerable change of the film chemistry and microstructural changes such as an amorphous to crystalline transition[21] take place in annealing after the deposition.

Gadolinia-Dopant Concentration in Ceria. The thin films analyzed in this study have a high Gd dopant

(30) Fallah, J. E.; Hilaire, L.; Romeo, M.; Le Normand, F. *J. Electron Spectrosc. Related Phenom.* **1995**, *73*, 89.
(31) Rupp, J. L. M.; Gauckler, L. J. *Solid State Ionics* **2006**, *177*, 2513−2518.
(32) Rupp, J. L. M.; Infortuna, A.; Gauckler, L. J. *J. Am. Ceram Soc.* **2006**, in press.

Table 7. XPS Analysis of the As-Deposited and Annealed Gadolinia-Doped Ceria Spray Pyrolysis Thin Films[a]

gadolinia-doped ceria thin film	at % Ce	at % Gd	at % O	at % Cl	at % C	Ce:Gd	(Ce + Gd):O
as-deposited	30.9	9.3	55.7	4.1	0	3.3	1.4
annealed at 1000 °C for 1 h (with 3 °C/min)	31.9	9.3	56.6	2.2	0	3.3	1.4

[a] Chemical analysis is shown for both thin films for a sputtering time that corresponds to a depth of 10 nm in SiO_2.

concentration of about 23 at %. The dopant dominates the electrical properties of the films, and the contributions of the residues from the precursors are negligible.[33] For the correct understanding and modeling of the processes taking place in thin-film solid oxide fuel cells based on doped ceria ceramics, it is of particular importance to know the spatial distribution of the dopant atoms. A detailed analysis of the depth profiles of the XPS spectra reveals that the dopant concentration does not depend on the depth in the film. Gd is distributed homogenously over the film cross section, as it was found to be constant after the first sputter cycle. Also, no difference in the cation distribution was found in either the annealed or as-deposited films. It can be concluded that the formation of the cerium gadolinium oxide is finished after the pyrolysis process.

A reduction of ceria from a mixed-valence state of Ce^{3+}/Ce^{4+} before sputtering to mainly Ce_2O_3 afterward is observed with increasing sputter time and sputtered depth. In previous XPS analysis on the ceria system, strong reduction effects were reported for long exposure to XPS X-rays sources[15,16,30] and for Ar^+ sputtering[34] in an ultrahigh vacuum. Pfau and Schierbaum argued that Ar^+ sputtering completely reduces CeO_2 to Ce_2O_3 with equal efficiency as hydrogen exposure.[34] Therefore, we assume that the reduction of ceria in CGO spray pyrolysis thin films with increasing sputter depth is induced by the Ar^+ sputtering and is not an original property of the film. A conclusion about the oxidation state of cerium in the bulk is not possible from our XPS analysis, because the application of Ar^+ for sputtering systematically changes the sample.

The presence of Ce_2O_3 or Gd_2O_3 doping in the CeO_2 host lattice results in the formation of point defects with oxygen vacancies and electrons as charge carriers. The electrical conductivity of gadolinia-doped ceria spray pyrolysis thin films is driven by its oxygen ion conductivity and the electronic conductivity via a "small polaron hopping" mechanism.[35] Concerning the electrical properties of the CGO spray pyrolysis thin films investigated here, we can assume a constant oxygen vacancy migration over the film thickness for oxygen vacancies resulting from the gadolinia dopant. However, information on the real oxidation state of the ceria gets lost because of the reducing influence of the Ar^+ sputtering, and it is unpredictable whether oxygen vacancies associated with the oxidation and reduction state of the ceria remain constant over the film thickness.

5. Conclusions

Gadolinia-doped ceria thin films synthesized with spray pyrolysis might be advantageous for achieving a reduction in the solid oxide fuel cell operating temperature because of the constant distribution of the dopant over the film thickness, the small thickness of 100−500 nm, and the dense microstructure. Once the first surface layer is sputtered by Ar^+, spray-pyrolyzed CGO thin films show a surprisingly stable and constant dopant concentration as a function of film thickness in XPS depth profiling experiments. Therefore, a constant oxygen ion vacancy migration over the film thickness can be assumed for applications like electrolyte films in solid oxide fuel cells.

The pyrolysis process is not completed during the spray pyrolysis deposition of gadolinia-doped ceria thin films at 350 °C. Residues of the spray pyrolysis precursors such as carbon from the organic solvents and chlorine and water from the used salts are even present after thermal treatment at 1000 °C. The residues accumulate in the topmost 10−20 nm of the thin film. The pyrolysis process of gadolinia-doped ceria spray-pyrolyzed thin films utilized as electrolytes in solid oxide fuel cells will be an ongoing process during the start-up and first operation hours, even at high operating temperatures such as 800−1000 °C. So far, the residues of the spray pyrolysis film observed here are not known to affect the electrical properties of gadolinia-doped ceria.

Supporting Information Available: Mass spectrometry results. This material is available free of charge via the Internet at http://pubs.acs.org.

CM061449F

(33) Tschope, A.; Kilassonia, S.; Birringer, R. *Solid State Ionics* **2004**, *173*, 57.
(34) Pfau, A.; Schierbaum, K. D. *Surf. Sci.* **1994**, *321*, 71.
(35) Tuller, H. L.; Nowick, A. S. *J. Phys. Chem. Solids* **1977**, *38*, 859.
(36) Raiser, D.; Deville, J. P. *J. Electron Spectrosc. Related Phenom.* **1991**, *57*, 91.